

Preparation of aluminum doped zinc oxide films and the study of their microstructure, electrical and optical properties

Hong-ming Zhou^{*}, Dan-qing Yi, Zhi-ming Yu, Lai-rong Xiao, Jian Li

School of Materials Science and Engineering, Central South University, Changsha, Hunan 410083, China

Received 25 November 2006; received in revised form 25 January 2007; accepted 26 January 2007

Available online 3 February 2007

Abstract

Aluminum doped zinc oxide (AZO) polycrystalline thin films were prepared by sol–gel dip-coating process on optical glass substrates. Zinc acetate solutions of 0.5 M in isopropanol stabilized by diethanolamine and doped with a concentrated solution of aluminum nitrate in ethanol were used. The content of aluminum in the sol was varied from 1 to 3 at.%. Crystalline ZnO thin films were obtained following an annealing process at temperatures between 300 °C and 500 °C for 1 h. The coatings have been characterized by X-ray diffraction, UV–Visible spectrophotometry, scanning electron microscopy, and electrical resistance measurement. The ZnO:Al thin films are transparent (~90%) in near ultraviolet and visible regions. With the annealing temperature increasing from 300 °C to 500 °C, the film was oriented more preferentially along the (0 0 2) direction, the grain size of the film increased, the transmittance also became higher and the electrical resistivity decreased. The X-ray diffraction analysis revealed single-phase ZnO hexagonal wurtzite structure. The best conductors were obtained for the AZO films containing 1 at.% of Al, annealed at 500 °C, 780 nm film thickness.

© 2007 Elsevier B.V. All rights reserved.

Keywords: Sol–gel; Zinc oxide films; Structural properties; Conductivity

1. Introduction

Aluminum doped zinc oxide (AZO) coatings exhibit high transparency and low resistivity and these materials are suitable for fabricating transparent electrodes in solar cells, gas sensors and ultrasonic oscillators [1–3]. They are also found in applications such as surface acoustic devices, optical waveguides and micro-machined actuators. They are an alternative material to tin oxide and indium tin oxide, which have been most used up to date [4–6].

ZnO thin films have been prepared by a variety of thin film deposition techniques, such as pulsed-laser deposition [7], RF magnetron sputtering [8–10], chemical vapor deposition [11], spray pyrolysis [12–14], chemical bath deposition [15] and the sol–gel process [16–25]. Among the preparation techniques of ZnO films, the sol–gel process in combination with the dip-coating process, offers the greatest possibility of preparing a small as well as large-area coating of ZnO thin films at low cost

for technological applications. A recent compilation of the properties of sol–gel derived AZO films is given in Ref. [23]. The reported resistivities vary from 7×10^{-4} to $10 \Omega \text{ cm}$ whereas the reported resistivities of sputtered films are as low as $1 \times 10^{-4} \Omega \text{ cm}$ [26,27]. In several studies, it was shown that the optical and electrical properties of AZO thin films could be obviously improved by optimized deposition conditions and doping [13,14]. Additionally, the opto-electrical properties of AZO thin films could be modified by thermal treatment in a reducing atmosphere [19]. The indium doped ZnO films grown at deposition temperature of 400 °C and 450 °C showed an improved crystallinity (exturization along the *c*-axis) which resulted in a strong decrease of the resistivity [28]. Ohyama reported that the use of 2-methoxyethanol and monoethanolamine, solvents with high boiling point, resulted in transparent ZnO films with strongly preferred orientation and that better electrical and optical properties had been obtained in 0.5 at.% aluminum doped ZnO thin films heated in reducing atmosphere [23,29]. Nunes found that when the doping concentrations of Al, In and Ga were 1, 1 and 2 at.%, respectively, electrical and optical properties of doped ZnO were superior [30].

^{*} Corresponding author. Tel.: +86 731 8830092.

E-mail address: ipezhm@yahoo.com.cn (H. Zhou).

The aim of this work is to investigate the influence of the preparation conditions on structural, electrical and optical properties of AZO films prepared by a non-alkoxide sol–gel method. The films were prepared from colloidal suspensions containing different Al concentrations and deposited by dip-coating on glass substrates. The structural characteristics were studied by X-ray diffraction (XRD), the morphological features were studied by scanning electron microscope (SEM), the film thickness was measured using surface-profilometry, and the electrical and optical properties were investigated by resistivity measurement and UV–Visible spectrophotometry (UV–Vis), respectively.

2. Experimental details

2.1. Preparation of sols

The preparation of the coating solution is shown in Fig. 1. The sol was prepared using zinc acetate dihydrate (ZnAc, Analytical grade, China), Diethanolamine (DEA, Analytical grade, China), and isopropanol (iPrOH, Analytical grade, China). DEA was first dissolved in isopropanol. Then zinc acetate dihydrate was added under stirring, and heated under reflux for 1 h at 70 °C. Doping of the solution was obtained by adding a 0.2 M solution of aluminum nitrate in ethanol. The molar ratios of dopant in the solution, [Al/Zn], were varied between 1 and 3%. Isopropanol was added to adjust the solution concentration to 0.5 mol/l of ZnAc. The molar ratio of DEA to ZnAc was maintained at 1.0. The solution was stirred at 70 °C for 2 h to yield a clear and homogeneous solution, which served as the coating solution after cooling to room temperature. The coating was usually made 1 day after the solution was prepared.

2.2. Preparation of films

ZnO:Al films were prepared by dip-coating 1.0 mm thick alkali free glass (AF45 DESAG, slide dimensions 25 × 80 mm²) at a withdrawal speed of 8 cm/min. Those dip glasses were

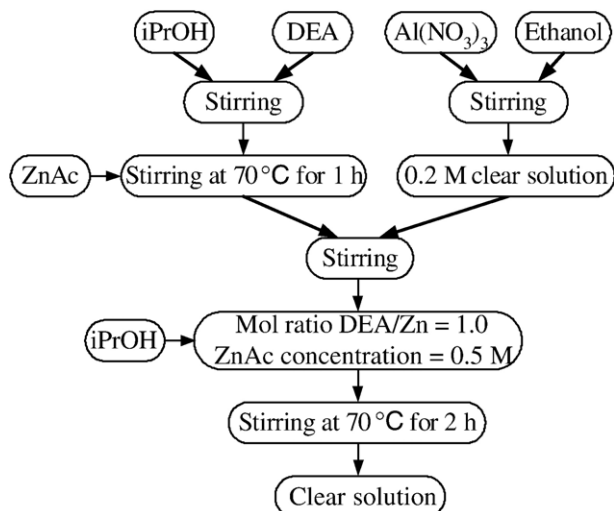


Fig. 1. Flow chart of the preparation of the coating solution.

cleaned with H₂SO₄/H₂O₂ solution and treated with a base solution (H₂O: NaOH, 29%: H₂O₂, 30% 5:1:1). After each coating the substrates were left in an oven at ~100 °C for 15 min, a precursor film on the substrate formed following the dip-coating process. The film was then dried at 240 °C for 1 min in a furnace (KSW-4D-11, China). Since the boiling point of DEA is 217 °C and the thermal decomposition temperature of ZnAc is 240 °C [31], a preheat treatment temperature of 240 °C is required for completely evaporating the solvent and removing organic residuals. Films were held in the horizontal position to avoid draining of the transferred sol, which could lead to different thickness in the coatings. The dipping was repeated up to 5, 10 and 20 times keeping the visual transparency of the coatings. During transfer, sols were kept in an ice bath.

2.3. Film annealing

As prepared films were heat treated in a furnace (KSW-4D-11, China) at 300–500 °C for 1 h in air atmosphere, to convert the organic coatings containing Zn²⁺ and Al³⁺ into their respective oxides. A heat ramp of 15 °C min⁻¹ was used and the samples were kept in the furnace until cooling to room temperature. Finally, a 400–1600 nm thick multilayered ZnO:Al film prepared under different deposition conditions was obtained and used for characterization.

2.4. Properties of AZO films

The crystallinity of each ZnO:Al film was determined by X-ray diffraction using an (Rigaku DMAX 2200, Japan) X-ray diffractometer with CuKα radiation source in the range of 20–70° with 0.02° step. The optical properties were studied by using a UV–Visible spectrophotometer (UV-2110, Japan). The surface morphology of the films was characterized by scanning electron microscope (LEO-1530, Germany). The SEM operating voltage is 20 kV. Film thickness was measured using a surface-profile recording meter (Surfcoeder SE30D, Japan). The electrical resistivity was measured by a four-point probe method; the expression was as follows [32].

$$\rho = \frac{\pi}{\ln 2} \left(\frac{\Delta V}{I} \right) W \quad (1)$$

where ρ is the electrical resistivity; ΔV is the potential difference of voltage probe; I is the current flow of current probe; W is the thickness of the coating.

3. Results and discussion

3.1. Structural properties

Fig. 2(a) shows the X-ray diffraction patterns of ZnO thin films doped with aluminum, whose concentration changes from 0 to 3 at.%. It can be seen from Fig. 2(a) that all samples are polycrystalline and exhibit the single-phase ZnO hexagonal wurtzite structure [33] (Joint Committee on Powder Diffraction Standards, 36–1451), all peaks in recorded range were identified.

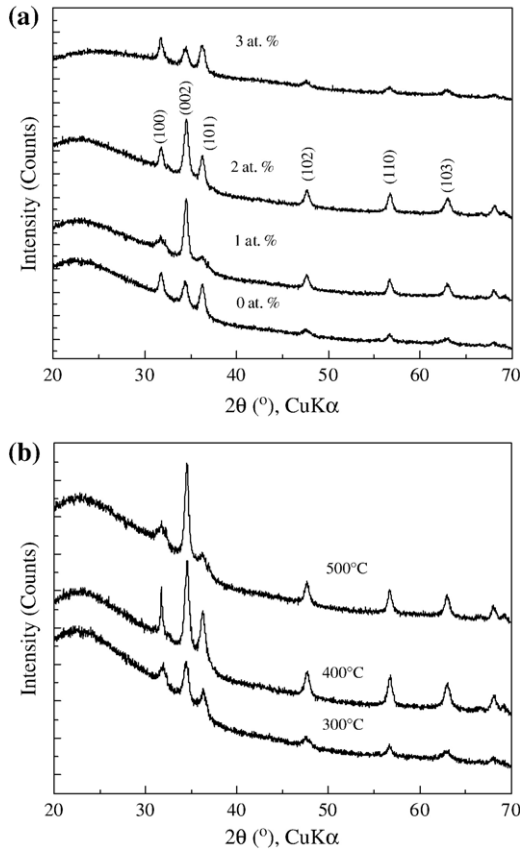


Fig. 2. X-ray diffraction patterns of the ZnO thin films with various aluminum concentrations (a) and annealing temperatures (b). The experimental conditions are: (a) annealing temperature: 500 °C; film thickness: 780 nm, (b) doping concentration: 1 at.%; film thickness: 780 nm).

Grains of undoped and doped films grow preferentially along the (0 0 2) plane. Film containing 1 at.% Al has the highest (0 0 2) diffraction peak intensity. Moreover, the peak intensities of those films decreased with doping concentrations increasing more than 1 at.%, which indicates that an increase in doping concentration deteriorates the crystallinity of films, which may be due to the formation of stress induced by ion size difference between zinc and aluminum and the segregation of aluminum in grain boundaries for high doping concentrations.

Fig. 2(b) indicates that the diffraction angles of all of AZO thin films are departed from 34.45° slightly which may be due to the doping of aluminum to zinc leading to the aberrance of ZnO crystal lattice. Moreover, both peak intensities and crystal size of those films increase with the increasing of annealing temperature, which may be due to the stresses decreasing with the increasing of annealing temperature. Furthermore, Fig. 2(b) also indicates that the crystallites are more oriented with the increasing of annealing temperature. We observed that the (0 0 2) peak is very sharp and other reflections appear relatively weak.

3.2. Morphology

The morphologies of ZnO thin films prepared from solution containing 0, 1 and 3 at.% aluminum as dopant are shown in Fig. 3. These SEM images show that the surface morphology of the films is strongly dependent on the concentration of aluminum. Uneven surface and dense microstructure are observed in Fig. 3 for the undoped ZnO film. The 1 at.% doped film exhibits a porous microstructure and the spherical crystalline particle size is approximately 30 nm. When the

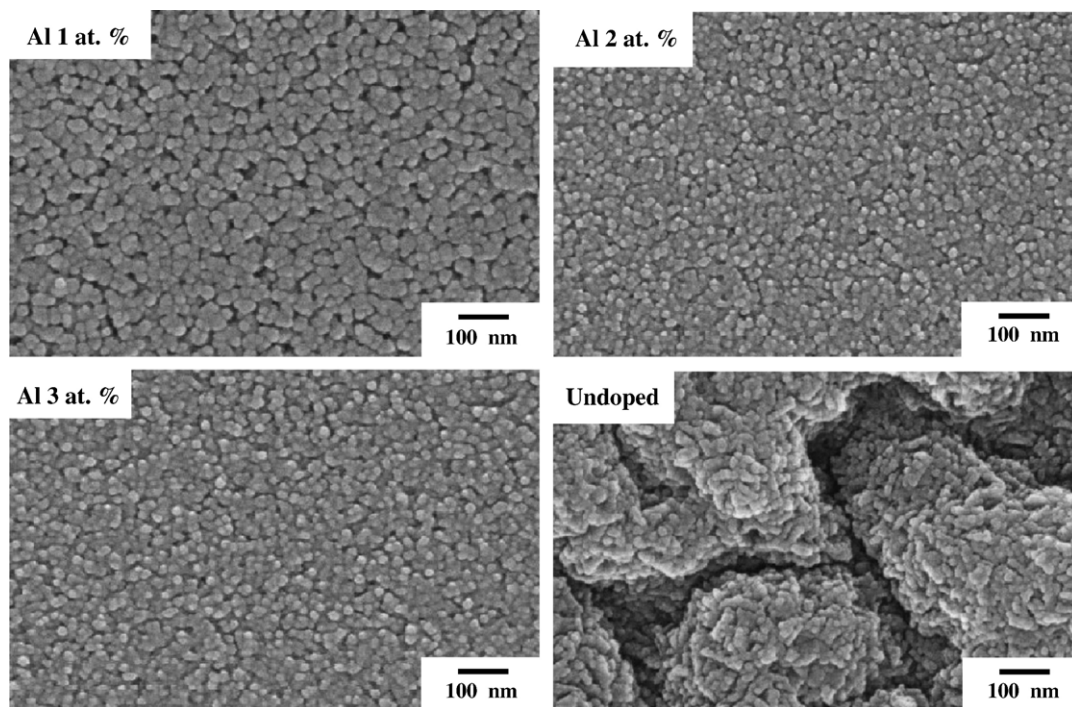


Fig. 3. SEM images of undoped and doped ZnO thin films with different aluminum contents. The experimental conditions are: annealing temperature: 500 °C; film thickness: 780 nm.

doping concentration is 2 at.%, particle size decreases and the film becomes denser. The surface morphology of 3 at.% doped film is similar to that of 2 at.% doped film. The change of particle size is due to a high difference in ionic radius between zinc (0.074 nm) and aluminum (0.057 nm) [30].

SEM images of aluminum-doped ZnO thin films annealed at different temperatures are shown in Fig. 4. It can be seen that, with the annealing temperature increasing from 300 °C to 500 °C, the particle size is increased and more voids are present in the film.

3.3. Optical properties

The effects of doping aluminum concentrations (a), annealing temperatures (b) and film thickness (c) on the optical transmittance spectra in the visible range of undoped and doped ZnO thin films are presented in Fig. 5.

Fig. 5(a) indicates that the transmittance of the doped and undoped ZnO films is always higher than 82% and the transmittance of the doped ZnO films is higher than that of the undoped films. Moreover, the transmittance of doped film with 1 at.% Al is near 90% for wavelengths over 400 nm, and is higher than that of the doped film with 2 at.% and 3 at.%. This may be due to the fact that the film with 1 at.% doping presents more voids than the films with 2 and 3 at.% doping, which may lead to a decrease in optical scattering.

It can be seen from Fig. 5(b) that, when the annealing temperature is increased from 300 °C to 500 °C, the

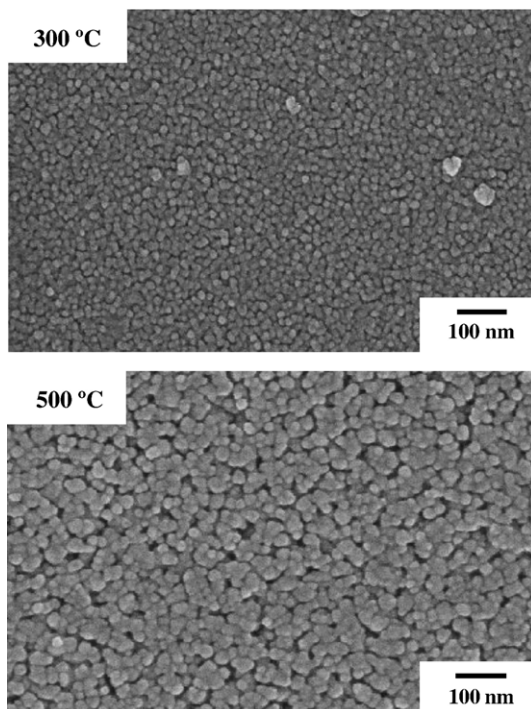


Fig. 4. SEM images of AZO thin films at different annealing temperatures. The experimental conditions are: doping concentration: 1 at.%; film thickness: 400 nm.

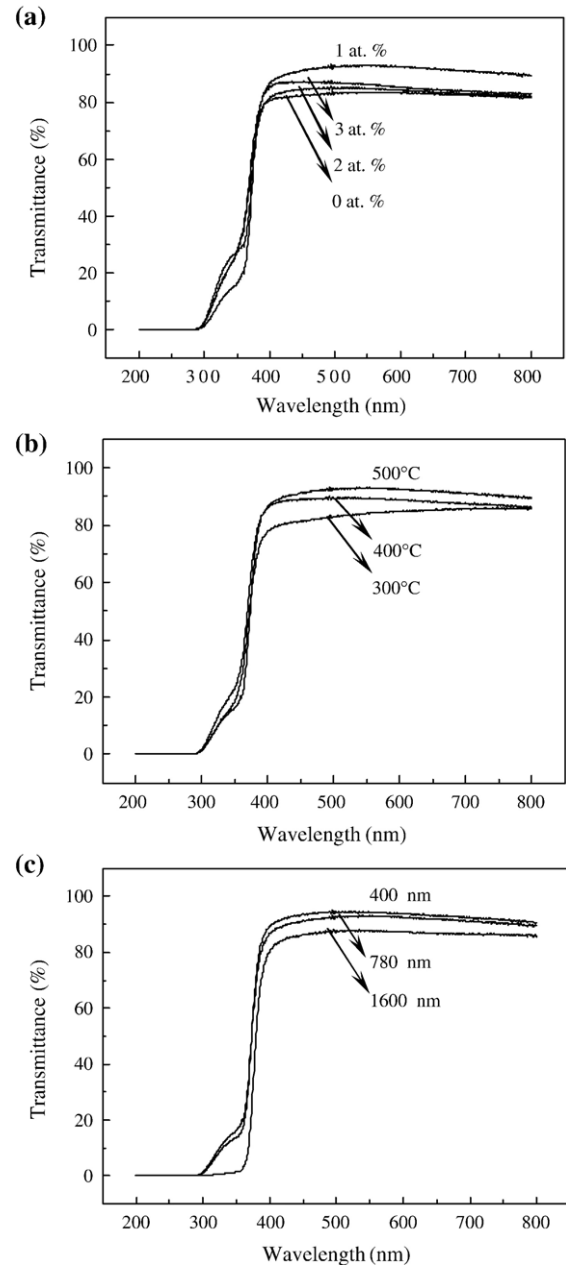


Fig. 5. The effects of doping aluminum concentrations (a), annealing temperatures (b) and film thickness (c) on the optical transmittance of the undoped and doped ZnO thin films. The experimental conditions are: (a) annealing temperature: 500 °C; film thickness: 780 nm, (b) doping concentration: 1 at.%; film thickness: 780 nm, (c) doping concentration: 1 at.%; annealing temperature: 500 °C.

transmittance of the AZO films increases. The transmittance of the AZO films annealed at 500 °C is higher than 90% for wavelengths over 400 nm. As mentioned before (Fig. 4), particle size and number of voids present in the film increase with increasing annealing temperature and may lead thus to a decrease in optical scattering.

Fig. 5(c) indicates that, when the thickness of the AZO films is increased from 400 nm to 1600 nm, the transmittance of the AZO films decreases gradually.

3.4. Electrical properties

Besides the optical properties, the electrical properties are also an important aspect of the performance of the AZO thin films. The effects of doping aluminum concentration (a), annealing temperatures (b) and film thickness (c) on the electrical resistivity of the doped and undoped ZnO thin films are presented in Fig. 6.

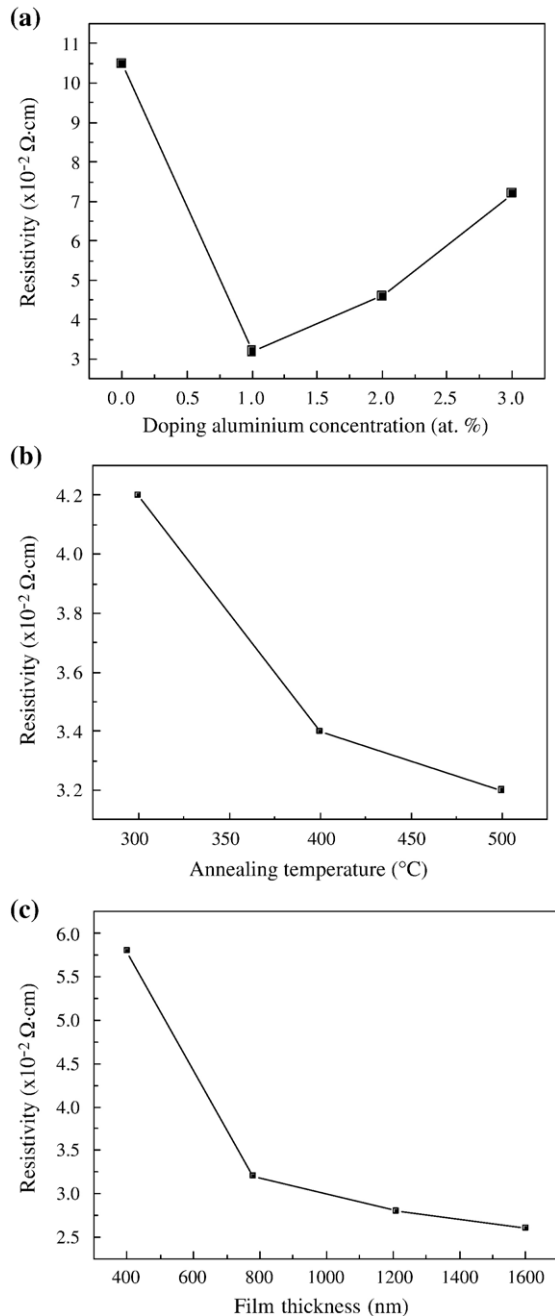


Fig. 6. The effects of doping aluminum concentration (a), annealing temperatures (b) and film thickness (c) on the electrical resistivity of the doped and undoped ZnO thin films. The experimental conditions are: (a) annealing temperature: 500 °C; film thickness: 780 nm, (b) doping concentration: 1 at.%; film thickness: 780 nm, (c) doping concentration: 1 at.%; annealing temperature: 500 °C.

The electrical conductivity of ZnO is directly related to the number of electrons, electrons formed by the ionization of the interstitial zinc atom and the oxygen vacancies [34]. It can be seen from Fig. 6(a) that, the electrical resistivity of the doped films is lower than that of the undoped films. The lowest electrical resistivity value of doped 1 at.% Al-doped film is $3.2 \times 10^{-2} \Omega \cdot \text{cm}$. However, the increase of the electrical resistivity of doped films with increasing doping concentration may be due to a decrease in mobility of the carriers caused by the segregation of the dopant at the grain boundary. Doped aluminum is acting as an electrical dopant at initial doping concentration but as an impurity at higher doping concentrations, the latter films having the lowest electrical resistivity values. Additionally, it has been shown that the electrical resistivity value of doped films is inversely proportional to the prevalence of the (0 0 2) orientation of film [19].

As mentioned above, the electrical resistivity of the films decreases with the increase of the (0 0 2) preferred orientation of the film, which is influenced by the annealing temperature (Fig. 2(a)). Fig. 6(b) shows the effect of annealing temperature on the electrical resistivity. The electrical resistivities of the films are decreased gradually with the increasing of annealing temperature, which may be attributed to the fact that the grain boundaries and the crystal lattice deficiencies of the film are decreased (Fig. 4) with the increasing of annealing temperature, resulting in an increase of the mobility of the carriers.

The increase of the film thickness will decrease electrical resistivity of the films, as a consequence, electrical resistivity variations of the films as a function of film thickness are plotted in Fig. 6(c). It can be seen from Fig. 6(c) that, the electrical resistivity values of the films decrease quickly when the film thickness increasing from 400 nm to 780 nm, then slowly down with the film thickness increases ulteriorly from 780 nm to 1600 nm. However, the transmittance of the 400 nm films is slightly higher than that of the 780 nm films, which is shown in Fig. 5(c). As a consequence, film thickness of 780 nm is preferred.

4. Conclusions

Al-doped zinc oxide transparent films (AZO) were prepared by a non-alkoxide sol–gel technique. when the annealing temperature was increased from 300 °C to 500 °C, the films were oriented more preferentially along the (0 0 2) direction, the grain size of the films increased, the transmittance also became higher and the electrical resistivities decreased. Films doped with 1 at.% Al had stronger orientation along the (0 0 2) direction, larger grain, higher conductivity and transmittance than that of the other doped films. In particular, the electrical resistivity of the 780-nm thick 1 at.% Al-doped ZnO film annealed at 500 °C reached $3.2 \times 10^{-2} \Omega \cdot \text{cm}$, while a transmittance over 90% in the visible range was achieved.

Acknowledgement

Financial support from the Postdoctoral Science Foundation of Central South University is gratefully acknowledged.

References

- [1] J. Nishino, T. Kawarada, S. Ohisho, H. Saitoh, K. Maruyama, K. Kamata, *J. Mater. Sci. Lett.* 16 (1997) 629.
- [2] M. Ritala, T. Asikainen, M. Leskelä, J. Skarp, *Mater. Res. Soc. Symp. Proc.* 426 (1996) 513.
- [3] R. Wang, L.L.H. King, W.W. Sleight, *J. Mater. Res.* 11 (1996) 1659.
- [4] V. Gupta, A. Mansingh, *J. Appl. Phys.* 80 (1996) 1063.
- [5] M.M. Bertolotti, M.V. Laschena, M. Rossi, A. Ferrari, L.S. Qian, F. Quaranta, A. Valentini, *J. Mater. Res.* 5 (1990) 1929.
- [6] T. Schuler, M.A. Aegerter, *Thin Solid Films* 351 (1999) 125.
- [7] S. Hayamizu, H. Tabata, H. Tanaka, T. Kawai, *J. Appl. Phys.* 80 (1996) 787.
- [8] J.A. Anna Selvan, H. Keppner, A. Shah, *Mater. Res. Soc. Symp. Proc.* 426 (1996) 497.
- [9] T. Nakada, N. Murakami, A. Kunioka, *Mater. Res. Soc. Symp. Proc.* 426 (1996) 411.
- [10] B. Szyszka, S. Jäger, *J. Non-Cryst. Solids* 218 (1997) 74.
- [11] J.L. Deschanvres, B. Bochu, J.C. Joubert, *J. Phys.* 4 (1993) 485.
- [12] C. Messaoudi, D. Sayah, M. Abd-Lefdil, *Phys. Status Solidi* 151 (1995) 93.
- [13] M.S. Tokumoto, A. Smith, C.V. Santilli, S.H. Pulcinelli, E. Elkaim, V. Briois, *J. Non-Cryst. Solids* 273 (2000) 302.
- [14] M.S. Tokumoto, A. Smith, C.V. Santilli, S.H. Pulcinelli, A.F. Craievich, E. Elkaim, A. Traverse, V. Briois, *Thin Solid Films* 416 (2002) 284.
- [15] P. O'Brien, T. Saeed, J. Knowles, *J. Mater. Chem.* 6 (1996) 1135.
- [16] T. Schuler, M.A. Aegerter, *Thin Solid Films* 351 (1999) 125.
- [17] M.S. Tokumoto, S.H. Pulcinelli, C.V. Santilli, A.F. Craievich, *J. Non-Cryst. Solids* 247 (1999) 176.
- [18] M.N. Kamalasanan, S. Chandra, *Thin Solid Films* 288 (1996) 112.
- [19] J.-H. Lee, B.-O. Park, *Thin Solid Films* 426 (2003) 94.
- [20] A.E. Jiménez González, J.A. Soto Urueta, *Sol. Energy Mater. Sol. Cells* 52 (1998) 345.
- [21] G.G. Valle, P. Hammer, S.H. Pulcinelli, C.V. Santilli, *J. Eur. Ceram. Soc.* 24 (2004) 1009.
- [22] R.F. Silva, M.E.D. Zaniquelli, *J. Non-Cryst. Solids* 247 (1999) 248.
- [23] M. Ohyama, H. Kozuka, T. Yoko, *J. Am. Ceram. Soc.* 81 (1998) 1622.
- [24] M. Ohyama, H. Kozuka, T. Yoko, *Thin Solid Films* 306 (1997) 78.
- [25] Y. Talahashi, M. Kanamori, A. Kondoh, H. Minoura, Y. Ohya, *Jpn. J. Appl. Phys.* 33 (1994) 6611.
- [26] W. Tang, D.C. Cameron, *Thin Solid Films* 238 (1994) 83.
- [27] H. Nanto, T. Minami, S. Shooji, S. Takata, *J. Appl. Phys.* 55 (1984) 1029.
- [28] B.E. Sernelius, K.F. Berggren, Z. Jin, I. Hamberg, C.G. Granqvist, *Phys. Rev.* 37 (1998) 10244.
- [29] M. Ohmyama, H. Kozuka, T. Yoko, *J. Ceram. Soc. Jpn.* 104 (1996) 296.
- [30] P. Nunes, E. Fortunato, P. Tonello, F. Braz Fernandes, P. Vilarinho, R. Martins, *Vacuum* 64 (2002) 281.
- [31] T.Q. Liu, O. Sakurai, N. Mizutani, M. Kato, *J. Mater. Sci.* 21 (1986) 3698.
- [32] F.M. Smith, *Bell Syst. Tech. J.* 37 (1958) 711.
- [33] Powder Diffraction Files, Joint Committee on Powder Diffraction Standards, ASTM, Philadelphia, PA, 1967 Card 36–1451.
- [34] M.H. Sukkar, H.L. Tuller, *Adv. Ceram.* 7 (1984) 71.